Static stress change from the 8 October, 2005 M = 7.6 Kashmir earthquake

Tom Parsons,[1] Robert S. Yeats,[2] Yuji Yagi,[3] and Ahmad Hussain[4]

[1] We calculated static stress changes from the devastating **M** = 7.6 earthquake that shook Kashmir on 8 October, 2005. We mapped Coulomb stress change on target fault planes oriented by assuming a regional compressional stress regime with greatest principal stress directed orthogonally to the mainshock strike. We tested calculation sensitivity by varying assumed stress orientations, target-fault friction, and depth. Our results showed no impact on the active Salt Range thrust southwest of the rupture. Active faults north of the Main Boundary thrust near Peshawar fall in a calculated stress-decreased zone, as does the Raikot fault zone to the northeast. We calculated increased stress near the rupture where most aftershocks occurred. The greatest increase to seismic hazard is in the Indus-Kohistan seismic zone near the Indus River northwest of the rupture termination, and southeast of the rupture termination near the Kashmir basin. **Citation:** Parsons, T., R. S. Yeats, Y. Yagi, and A. Hussain (2006), Static stress change from the 8 October, 2005 M = 7.6 Kashmir earthquake, *Geophys. Res. Lett.*, *33*, L06304, doi:10.1029/2005GL025429.

1. Introduction

[2] Kashmir shook violently on October 8th, 2005, when a **M** = 7.6 earthquake caused more than 87,000 deaths while making millions more homeless. The earthquake occurred in the Indus-Kohistan seismic zone [*Armbruster et al.*, 1978; *Seeber and Armbruster*, 1979] (Figure 1) with its epicenter in the Kishenganga (Neelam) Valley. The event was accompanied by rupture of the Balakot-Bagh fault along the Jhelum River near and southeast of Muzaffarabad and farther northwest near the town of Balakot in the North-West Frontier Province of Pakistan. The surface geology at the epicenter is the Kashmir syntaxis where the Main Boundary fault makes a hairpin turn from NW to S (Figure 1). The earthquake does not appear to have been influenced by these inactive [*Nakata et al.*, 1991] surface structures, but instead followed a northwest-southeast trending line of historical large earthquakes within the Himalaya as described by *Seeber and Armbruster* [1979] and continuing southeast into India where the zone of seismicity coincides with the topographic break between the Lesser Himalaya and Greater Himalaya [*Baranowski et al.*, 1984].

[3] The Indus-Kohistan seismic zone is continuous with a zone of seismicity along the Himalaya related to a ramp in the Main Himalayan thrust décollement that contributes to uplift of the High Himalaya [*Yeats et al.*, 1992; *Bilham*, 2004]. The Indus-Kohistan seismic zone continues northwest across Kashmir into the North-West Frontier Province of northern Pakistan. The NEIC and USGS fault-plane solutions for the 8 October event also show this northwest strike.

[4] In this paper we calculate coseismic static stress changes associated with the Kashmir earthquake in the context of known active faults in the region. Coseismic stress changes have been useful in identifying locations of future large earthquakes [e.g., *Stein et al.*, 1997; *Nalbant et al.*, 2005]. Under a renewal model of earthquakes, we expect a static stress increase to raise the probability of an earthquake by reducing its time to failure [e.g., *Working Group on California Earthquake Probabilities*, 1990].

2. Method

[5] We calculated coseismic static stress change by simulating an earthquake with a slipping dislocation in an elastic half space [e.g., *Okada*, 1992]. Changed stress tensor components were resolved on planes of interest and related to triggering or inhibition of future earthquakes. Usually a Coulomb failure criterion is calculated to explain patterns of seismicity change [e.g., *Harris*, 1998, and references therein]. The Coulomb criterion ($\Delta\tau$) is defined by

$$\Delta\tau \equiv \left|\Delta\overline{\tau}_f\right| + \mu'(\Delta\sigma_n - \Delta p) \qquad (1)$$

where $\Delta\overline{\tau}_f$ is the change in shear stress on the receiver fault (set positive in the direction of fault slip), μ is the coefficient of friction, $\Delta\sigma_n$ is the change in normal stress acting on the target fault (set positive for unclamping), and Δp is pore pressure change.

[6] To simulate the Kashmir earthquake, we needed to estimate its coseismic slip distribution (Figure 2). The spatial and temporal slip distribution of the Kashmir earthquake was inverted from 32 teleseismic body waveforms (P-wave). Teleseismic body waves were windowed for 80 s, starting 10 s before the first motion, bandpassed between 0.01 and 1.0 Hz, and then converted into ground displacement with a sampling time of 0.2 s. We used a numerical method for the multi-time window inversion scheme [e.g., *Yoshida*, 1992; *Yagi et al.*, 2004]. Following previous studies, we represented the rupture as a spatiotemporal slip distribution on a plane. Slip was resolved on a single source fault 125 km long and 25 km wide, which was divided into 5x5 km patches. The slip-rate function on each patch was expanded into a series of 7 triangle functions with a rise

---

[1]U.S. Geological Survey, Menlo Park, California, USA.
[2]Department of Geosciences, Oregon State University, Corvallis, Oregon, USA.
[3]Graduate School of Life and Environmental Sciences, University of Tsukuba, Tsukuba, Japan.
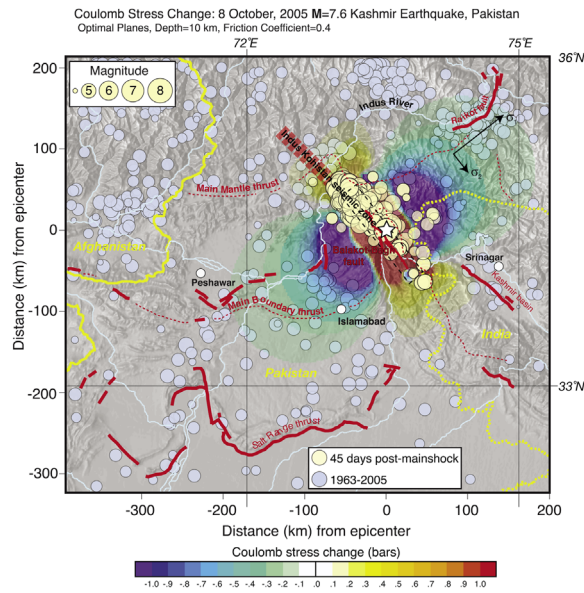[4]Geological Survey of Pakistan, Peshawar City, Pakistan.

Figure 1. Coulomb stress change on optimally oriented fault planes at 10 km depth from the 8 October, 2005 **M** = 7.6 Kashmir earthquake (epicenter shown by star). Optimal orientations were calculated using principal stress vectors shown at upper right, and we used a friction coefficient of 0.4 (parameter sensitivity of calculations is shown in Figures 3 and 4). The outer edges of the source dislocation is shown by the dashed black rectangle. Surface rupture is shown with a red line and is from Geological Survey of Pakistan mapping. The Indus-Kohistan seismic zone of *Armbruster et al.* [1978] is shown with a heavy dashed red line extending northwest of the mainshock rupture zone. Blue dots show 1963-2005 earthquake activity. Aftershocks from the first 45 days after the mainshock are shown with yellow dots. Active faults are identified by heavy red lines [*Yeats et al.*, 1992], and inactive faults are finer dashed red lines.

time of 1 s. A rupture front velocity was set at 3.2 km/s, which gave a start time of the basis function at each subfault. We calculated Green's functions for teleseismic body waves using the method of *Kikuchi and Kanamori* [1991] with the standard Jeffreys-Bullen's crustal structure, and solved the least squares problem with weak constraint of smoothness on slip distribution. The slip direction was also constrained between reference rake of ±45° by using the nonnegative least squares algorithm by *Lawson and Hanson* [1974]. Since the hypocentral depth was not adequately constrained by the global seismological network, we varied it in the inversion using two possible fault planes and found a hypocentral depth of 9km, with a strike of 331°, dip of 31°, and a reference rake of 108°; a minimum variance of 0.29 in the waveform inversion was achieved with these parameters.

[7] To make Coulomb stress change calculations, one must resolve stress components on defined planes of interest; additionally, estimates of target fault friction coefficient and some means of treating pore fluid pressure must be developed. Here we calculated stress changes on optimally oriented fault planes, as defined by an assumed regional stress direction, using the method of *Toda et al.*

[1998]. There is ample evidence of a regional compressive stress field near the Himalayan front, and we defined a greatest principal stress direction as orthogonal to the strike of the 8 October **M** = 7.6 Kashmir earthquake rupture plane (Figure 1). This direction roughly characterizes the Indus-Kohistan seismic zone trend, which is a primary structure of interest in terms of potential large earthquake occurrence. We investigated sensitivity of our results to regional stress orientation (Figure 3) by making sample calculations with horizontal principal stresses (σ_1 and σ_2) orientations rotated by ±45° from the preferred N61°E direction (of σ_1) shown in Figure 1.

[8] We allowed an assumed regional stress field to define target fault orientation and rake, but we did not know the frictional state, pore fluid pressure, or nucleation depth on these potential faults. Commonly, Skempton's coefficient B_k (which varies from 0 to 1) is used to incorporate pore fluid effects, where the effective coefficient of friction $\mu' = \mu(1 - B_k)$ is adjusted and used in the Coulomb failure criterion as $\Delta\tau \equiv |\Delta\overline{\tau}_f + \mu'(\Delta\sigma_n)$ after *Rice* [1992]. Thus variation of the effective friction coefficient can serve as a proxy for treating pore fluid pressure, although this should be recognized as an oversimplification [e.g., *Beeler et al.*, 2000].

[9] The stress change map shown in Figure 1 was calculated with a friction coefficient of μ = 0.4 at 10 km depth. We varied target-fault friction coefficient from μ = 0 to μ = 0.8, and depths from 5 to 15 km to test effects of parameter uncertainties. We found sensitivity in the results to parameter choices, but not to the degree that altered the sign of the calculated stress change at specific target fault zones, or that changed the general pattern of stress change (Figure 4).

3. Interpretation of Calculated Stress Changes in the Kashmir Region

[10] We examined stress transfer effects from the 8 October 2005 **M** = 7.6 Kashmir earthquake on regional active faults. Major structures along the Himalayan front include the inactive Main Mantle and Main Boundary thrusts; *Madin et al.* [1989] and *Yeats et al.* [1992] showed evidence for reactivation along parts of these structures, including part of the 8 October 2005 source fault (Figure 1). Range-front faulting is active south of the Main Boundary thrust on the Salt Range thrust, a complex zone of strike-
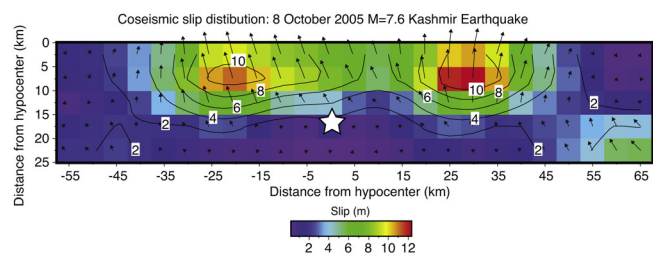

Figure 2. Coseismic slip distribution of the 8 October, 2005 **M** = 7.6 Kashmir earthquake (hypocenter shown by star). The source dislocation used in static stress calculations was developed with the same 5x5 km discretization as shown. Each patch has a specified rake as shown by the vectors, which are scaled by slip magnitude.
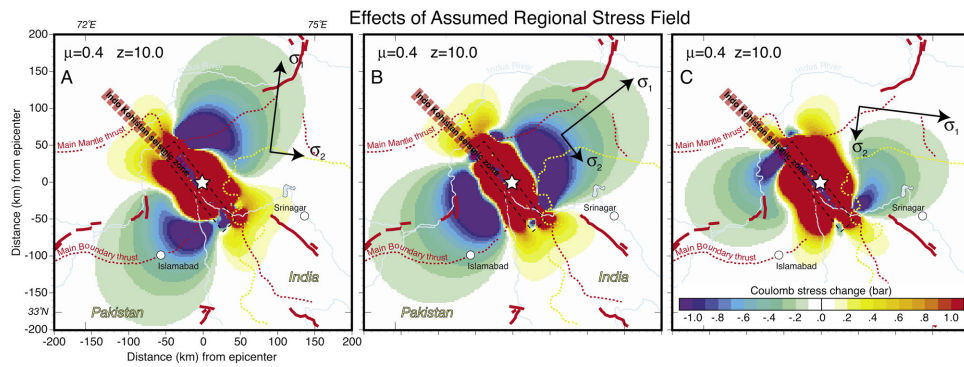
Figure 3. Sensitivity of stress-change calculations to regional stress orientations. (a) The greatest (σ_1) and intermediate (σ_2) principal stresses are rotated 45° counterclockwise from orthogonal and (b) perpendicular to the 8 October 2005 earthquake strike. (c) Stress orientations are rotated 45° clockwise.

slip and thrust faulting [*Yeats et al.*, 1984]. The Indus-Kohistan seismic zone trends northwest from the end of the 8 October 2005 surface rupture, but lacks a mapped surface expression. The seismic zone was identified from micro-seismicity that defined a northwest-striking, northeast-dipping plane [*Armbruster et al.*, 1978] similar to that of the 8 October 2005 event. In this section we examine static stress change effects with respect to aftershock locations, and in the vicinity of known active faults.

[11] Calculated Coulomb stress-change patterns showed consistent features regardless of friction coefficient and depth (Figure 4). Stress-increased zones were confined to areas near, and off the ends of the rupture, while stress-decreased areas were located southwest and northeast of the rupture plane (Figure 1). Aftershocks ($\mathbf{M} \geq 4$, first 45 days) are plotted on Figure 1; for the most part, aftershocks were located within the stress-increased region. Taken by itself,

this observation may not be very meaningful since aftershocks are almost always most numerous on and near mainshock rupture planes. Perhaps more interesting is the correspondence between stress-decreased areas and lower aftershock rates. Forty-five days after the mainshock, just 6% of aftershocks had occurred in stress-decreased zones southwest and northeast of the mainshock contain despite the presence of active faults and past earthquake activity (Figure 1).

[12] Here we discuss known active faults in the region from south to north. We found that the Salt Range thrust lies out of reach of static stress effects of the 8 October 2005 event; calculated stress changes were less than 0.1 bars, the lower threshold for earthquake triggering shown by previous studies [e.g., *Reasenberg and Simpson*, 1992; *Hardebeck et al.*, 1998; *Harris*, 1998]. A series of active faults north of Peshawar and extending northeast to the
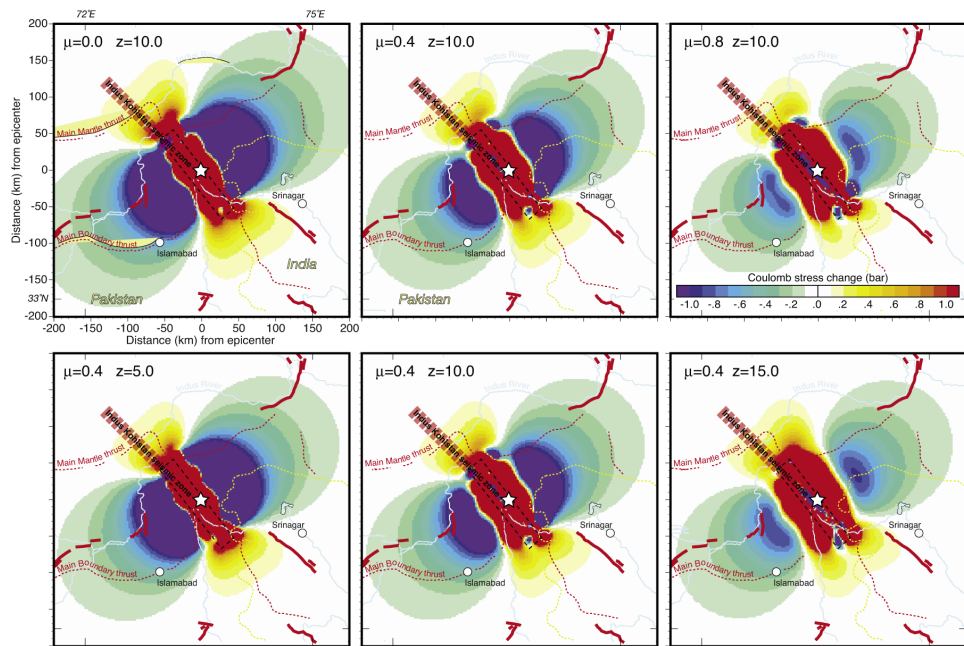

Figure 4. Sensitivity of Coulomb stress change calculations to friction coefficient and target-fault depth. Friction varied from $\mu = 0$ to $\mu = 0.8$ and depth ranged between 5 and 15 km. Differences are evident, but the overall stress-change pattern is consistent.

Indus River at Tarbela Dam [*Yeats and Hussain*, 1989] (near where a **M** = 6.7 earthquake occurred in 1878 [*Ambraseys and Douglas*, 2004]) fall within a calculated stress-decreased zone. We therefore do not consider these faults likely candidates for earthquake triggering. However, to the east, active faults in the Kashmir basin (near Srinagar in Indian controlled Kashmir) lie at the edge of a calculated stress-increased zone (Figure 1). This zone is also the site of an 1885 **M** = 6.3 event and possibly a much larger shock in 1555 [*Bilham*, 2004]. This zone might extend southeast as far as the nucleation site of the 1905 **M** = 7.8 Kangra earthquake, where a slip deficit still exists [*Wallace et al.*, 2005]. Calculated stress increase in the Kashmir basin area is sensitive to parameter choices because the basin lies near the edge of a stress-increased zone (Figures 3 and 4).

[13] There are two primary active fault zones near the north end of the 8 October 2005 rupture. The northwest extension of the Indus-Kohistan seismic zone (site of the 1974 **M** = 6.2 Pattan earthquake [*Pennington*, 1989]) lies in a stress-increased area and has already shown productive aftershock activity (Figure 1). Northeast of the 2005 earthquake, the Raikot fault zone lies in a calculated stress-decreased zone. This fault and surroundings has had frequent **M** ≤ 5.5 earthquakes in the past (Figure 1) and over time, might offer a test of the stress shadow hypothesis, where a seismicity rate decrease is expected from a static stress decrease.

4. Conclusions

[14] Changes in stress distribution caused by the 8 October 2005 **M** = 7.6 Kashmir earthquake might reasonably be associated with changes in seismic hazard. Our mapping of Coulomb stress changes on optimally oriented faults showed increased stress northwest of the rupture along the trend of the Indus-Kohistan seismic zone. A stress increase was also calculated southeast of the rupture near the Kashmir basin; faults in this region may have participated in large earthquakes in 1555 and 1885 [*Bilham*, 2004]. We calculated decreased stress in large regions southwest and northeast of the 2005 rupture, possibly delaying activity on active faults north the Main Boundary thrust near Peshawar and Tarbela Dam, and on the Raikot fault near the Main Mantle thrust.

References

Ambraseys, N. N., and J. Douglas (2004), Magnitude calibration of north Indian earthquakes, *Geophys. J. Int.*, *159*, 165–206.

Armbruster, J., L. Seeber, and K. H. Jacob (1978), The northwestern termination of the Himalayan mountain front: Active tectonics from microearthquakes, *J. Geophys. Res.*, *83*, 269–282.

Baranowski, J., J. Armbruster, L. Seeber, and P. Molnar (1984), Focal depths and fault plane solutions of earthquakes and active tectonics of the Himalaya, *J. Geophys. Res.*, *89*, 6918–6928.

Beeler, N. M., R. W. Simpson, S. H. Hickman, and D. A. Lockner (2000), Pore fluid pressure, apparent friction, and Coulomb failure, *J. Geophys. Res.*, *105*, 25,533–25,542.

Bilham, R. (2004), Earthquakes in India and the Himalaya: Tectonics, geodesy and history, *Ann. Geophys.*, *47*, 839–858.

Hardebeck, J. L., J. J. Nazareth, and E. Hauksson (1998), The static stress change triggering model: Constraints from two southern California earthquake sequences, *J. Geophys. Res.*, *103*, 24,427–24,437.

Harris, R. A. (1998), Introduction to special section: Stress triggers, stress shadows, and implications for seismic hazard, *J. Geophys. Res.*, *103*, 24,347–24,358.

Kikuchi, M., and H. Kanamori (1991), Inversion of complex body waves-III, *Bull. Seismol. Soc. Am.*, *81*, 2335–2350.

Lawson, C. L., and R. J. Hanson (1974), *Solving Least Squares Problems*, 340 pp., Prentice-Hall, Upper Saddle River, N. J.

Madin, I. P., R. D. Lawrence, and S. ur-Rehman (1989), The northwestern Nanga Parbat-Haramosh massif; Evidence for crustal uplift at the northwestern corner of the Indian craton, *Geol. Soc. Am. Spec. Pap.*, *232*, 169–182.

Nakata, T., H. Tsutsumi, S. H. Khan, and R. D. Lawrence (1991), Active faults of Pakistan, map sheets and inventories, *Spec. Publ. 21*, 141 pp., Hiroshima Univ. Res. Cent. for Reg. Geogr., Hiroshima, Japan.

Nalbant, S. S., S. Steacy, K. Sieh, D. Natawidjaja, and J. McCloskey (2005), Updated earthquake hazard in Sumatra, *Nature*, *435*, 756–757.

Okada, Y. (1992), Internal deformation due to shear and tensile faults in a half-space, *Bull. Seismol. Soc. Am.*, *82*, 1018–1040.

Pennington, W. D. (1989), A summary of field and seismic observations of the Pattan earthquake—28 December 1974, in *Geodynamics of Pakistan*, edited by A. Farah and K. A. DeJong, pp. 143–147, Geol. Surv. of Pakistan, Quetta.

Reasenberg, P. A., and R. W. Simpson (1992), Response of regional seismicity to the static stress change produced by the Loma Prieta earthquake, *Science*, *255*, 1687–1690.

Rice, J. R. (1992), Fault stress states, pore pressure distributions, and the weakness of the San Andreas Fault, in *Fault Mechanics and Transport Properties of Rocks: W. F.: A Festschrift in Honor of Brace*, edited by B. Evans and T. Wong, pp. 475–503, Elsevier, New York.

Seeber, L., and J. G. Armbruster (1979), Seismicity of the Hazra arc in northern Pakistan: Decollement vs. basement faulting, in *Geodynamics of Pakistan*, edited by A. Farah and K. A. DeJong, pp. 131–142, Geol. Surv. of Pakistan, Quetta.

Stein, R. S., A. A. Barka, and J. H. Dieterich (1997), Progressive failure on the North Anatolian fault since 1939 by earthquake static stress triggering, *Geophys. J. Int.*, *128*, 594–604.

Toda, S., R. S. Stein, P. A. Reasenberg, J. H. Dieterich, and A. Yoshida (1998), Stress transferred by the 1995 M_w = 6.9 Kobe, Japan, shock: Effect on aftershocks and future earthquake probabilities, *J. Geophys. Res.*, *103*, 24,543–24,565.

Wallace, K., R. Bilham, F. Blume, V. K. Gaur, and V. Gahalaut (2005), Surface deformation in the region of the 1905 Kangra Mw = 7.8 earthquake in the period 1846–2001, *Geophys. Res. Lett.*, *32*, L15307, doi:10.1029/2005GL022906.

Working Group on California Earthquake Probabilities (1990), Probabilities of large earthquakes in the San Francisco Bay region, California, *U.S. Geol. Surv. Circ.*, *1053*, 51 pp.

Yagi, Y., T. Mikumo, J. Pacheco, and G. Reyes (2004), Source rupture process of the Tecoma'n, Colima, Mexico earthquake of 22 January 2003, determined by joint inversion of teleseismic body-wave and near-source data, *Bull. Seismol. Soc. Am.*, *94*, 1795–1807.

Yeats, R. S., and A. Hussain (1989), Zone of late Quaternary deformation in the southern Peshawaar basin, Pakistan, *Geol. Soc. Am. Spec. Pap.*, *232*, 265–274.

Yeats, R. S., S. H. Khan, and M. Akhtar (1984), Late Quaternary deformation of the Salt Range of Pakistan, *Geol. Soc. Am. Bull.*, *95*, 958–966.

Yeats, R. S., T. Nakata, A. Farah, M. Fort, M. A. Mirza, M. R. Pandey, and R. S. Stein (1992), The Himalayan frontal fault system, *Ann. Tecton.*, *VI*, 85–98.

Yoshida, S. (1992), Waveform inversion for rupture process using a nonflat seafloor model: Application to 1986 Andreanof Islands and 1985 Chile earthquake, *Tectonophysics*, *211*, 45–59.

———————————
A. Hussain, Geological Survey of Pakistan, Peshawar City, Pakistan.

T. Parsons, U.S. Geological Survey, Menlo Park, CA 94025, USA. (tparsons@usgs.gov)

Y. Yagi, Graduate School of Life and Environmental Sciences, University of Tsukuba, Tsukuba 305-0802, Japan.

R. S. Yeats, Department of Geosciences, Oregon State University, Corvallis, OR 97331-5506, USA.